

Experimental study of variable idle speed control for an in-wheel electric vehicle drive

Ping Xiong* and Chenglin Gu

State Grid Hubei Electric Power Research Institute, and Huazhong University of Science and Technology, Wuhan 430074, P.R. China.

**Email: joey.xiongping@gmail.com; Corresponding Author.*

ABSTRACT

A new type clutch device is integrated into the drive train of a wheel drive electric vehicle to realize a flexible connection between the hub and the motor. Unlike the internal combustion engine (ICE), which has a minimal rotational speed, the electric motor is capable of idling at variable speeds. Then, a start-up mode for such a novel in-wheel drive system is proposed, which separates the motor starting and the load operation. Firstly, a simplified model of the drive train system is studied, and the performance indices for evaluating vehicle start-up are introduced. Afterwards the proposed starting method is investigated, and the idle speed is optimally tuned for finding a balance between the discontinuity of the wheel acceleration and the desired motor torque at the moment of clutch closure. Finally, the experiments are conducted on a laboratory test bench, and the results validate the improved comfort level and the enhanced torque capacity by applying the variable idle speed control strategy, compared with the obtained results by using the fixed idle speed control.

Keywords: clutch coupling; comfort level; fixed idle speed; optimal idle speed; start-up.

INTRODUCTION

Electric vehicle (EV) has been significantly developed around the world nowadays because of its prominent merits, e.g., zero-emission, low-noise, and low maintenance (Chan et al., 2010; Sultana et al., 2018). Among various types of existing EVs, the in-wheel drive mode becomes a preferred choice on account of its simple chassis, increased efficiency, reduced noise, flexible control, and so on (Xue et al., 2010; Larminie & Lowry, 2004). A fastened connection is commonly adopted between the motor and the hub. In the case of accelerating the vehicle from standstill, a large output torque of the driving motor is necessary to overcome the resistance torque arisen by the multi-factors as the bearing friction, the deformation of the wheel, roadbed, etc. (Heißing & Ersoy, 2011). For this reason, the excessive currents are essential under such starting conditions, which at times lead to overloading of the power source and a sudden reduction in the power to the driving motor. As a result, it would accelerate aging of car batteries and decrease reliability of vehicle start-up. In addition, the counter electromotive force caused by cutting off the power supply may damage the controllers while the EV implements the braking operation at a high speed (Wen et al., 2012). Consequently, the starting performances are not satisfactory under the existing drives, which are rigidly fastened, especially at urgent starting and braking.

A flexible connection between the output shaft of an engine and the input shaft of a transmission has been adopted to enhance the comfort level during starting or gear shifting in traditional gasoline automobiles. The design of clutch engagement controllers for automatic mechanical transmission (AMT) is extensively investigated in literatures, resulting in several solutions. The coordination between friction work of the single plate clutch and the shock intensity is optimized based on modern control theory. The decoupled controller (Jin et al., 2013), extreme value theorem (Lu et al., 2012), and model predictive control (MPC) controller (Yuan & Chen, 2013) are, respectively, designed for optimizing the displacement track of clutch and the engine throttle. Additionally, a centrifugal clutch is utilized to assist with motor starting under load. The centrifugal principle makes it possible to engage or disengage the load automatically at a pre-determined speed (Zhong et al., 2000). Also, the inclusion of a clutch mechanism within a vehicle's drive train results in a reduction in frictional losses and improves fuel economy in vehicles while coasting (Asmis & Schaffeld, 2012).

Referring to the experience of using the clutch to remit mechanical and electromagnetic shocks, a novel clutch device (unit) is used to disengage the hub motor from the wheel at starting or braking. Taking into account the restricted space between the motor and the hub, the clutch device is specially designed. Its operating principle, optimal structure design, and integration design of the clutch system for the in-wheel drive application are studied in previous work (Cai et al., 2015; Yu & Gu, 2017). A prototype for the in-wheel motor drive that includes such novel clutch units is demonstrated in Fig. 1. The motor torque is directly transmitted to the wheel after the push rods enter the slots of the joint holes, as displayed in Fig. 1(b). A set of clutch units are placed on the external surface of the outer rotor, which functions like a dog clutch for delivering or interrupting the power from the motor (master side) to the wheel (slave side). Correspondingly, the separable starting process between the motor and the wheel is defined as 'clutch start', whereas the starting process with a fastened connection between the motor and the wheel is defined as 'direct start'. Also, the preliminary studies of the clutch start and its numerical simulations have been disclosed, according to (Xiong & Gu, 2014).

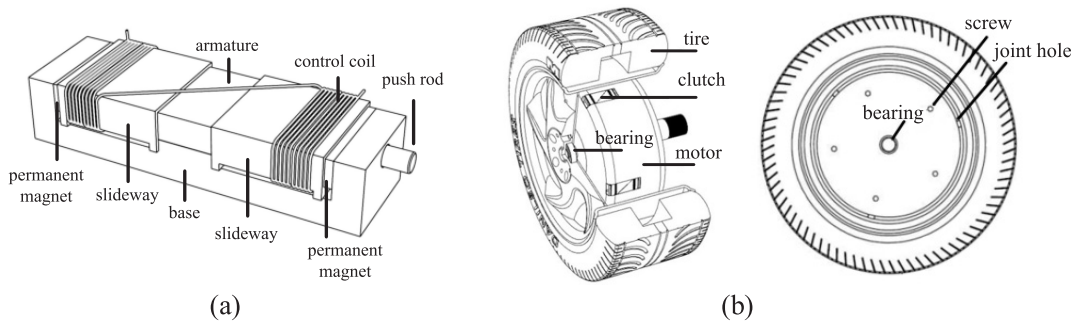


Figure 1. (a) A novel clutch device. (b) Assembly of the clutch units between the wheel and the motor.

The start-up mode that relates to the clutch operation can be captured in the same control manner. However, the automatic clutch that works on the centrifugal principle generally engages at a fixed idle speed. Subject to the minimum rotational speed of ICE, engine flameout may be caused via the operation of the abrupt engagement of the clutch. Feelings of discomfort will equally be experienced by drivers when the clutch engages with an inadequate speed difference (Matsushima, 2010). On the other hand, most of the controllers for clutch engagement are sensitive to the parameters, as the friction coefficient of clutch discs, time constant of actuator dynamics, etc., somehow increasing the complexity of controller design.

Owing to the adjustable-speed drive of the electric machine, the paper proposes a new solution for EV drive highlighted with the possibilities of 'no-load starting, variable-idle shifting, stepless speed changing, detached braking' together. Based on the action of the rapid clutch engagement between the master and slave sides of the drive train system, an ideal clutch model that conforms to the principle of impulse theorem between the two rotating mass is considered in this article. According to the presented simplified model, the investigations on the clutch start and its principle of idle speed selection are conducted. In summary, the main contributions are as follows:

- (1) design of a separable starting process between the motor and the wheel;
- (2) elaborating a control strategy for fast and smooth clutch engagement that is tunable with idle speeds.

ELECTRIC DRIVE TRAIN SYSTEM MODEL

In this research, we focus on the modeling of the driving motor, the clutch operation, and the vehicle resistance, thereby skipping influences of the wheel slip. A combined lumped mass model is used to estimate the dynamics of the drive train system. The schematic overview of the drive train system is shown in Fig. 2.

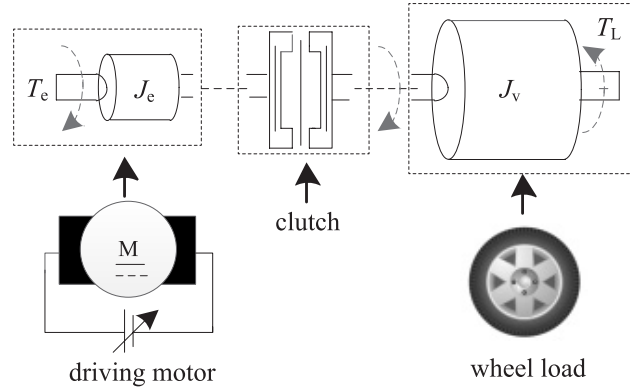


Figure 2. Schematic diagram of the simplified drive train system.

ELECTRIC MOTOR MODELING

Because the power supply from car battery is DC source, DC motor is selected for the traction of the entire drive train system. Accordingly, the mathematical model of DC motor can be described by the following equations:

$$L_a \frac{di_a}{dt} + i_a R_a + K_e \omega_e = u_a \quad (1)$$

$$J_e \frac{d\omega_e}{dt} = T_e - T_L \quad (2)$$

where u_a is the given armature voltage, J_e is the moment of inertia of DC motor, ω_e is the mechanical angular velocity, i_a is the armature current, R_a is the armature resistance, L_a is the armature inductance, K_e is the back electromotive force (emf) constant, T_e is the driving torque from DC motor, and T_L is the load torque.

VEHICLE RESISTANCE MODELING

In general, four major forces are associated with vehicle dynamics: rolling resistance, aerodynamic drag, grade force, and inertial resistance. Aerodynamic drag is considerably small enough to be neglected, compared with rolling resistance at starting moment. Combining Equation (1) and Equation (2), the overall model of the wheel drive EV system can be rewritten as

$$L_a \frac{di_a}{dt} + i_a R_a + K_e \omega_e = u_a \quad (3)$$

$$(J_e + J_v) \frac{d\omega_e}{dt} = K_T i_a - \frac{r_w}{G} (\mu M_v g + M_v g \sin \theta)$$

where M_v is the mass of EV, g is the gravity acceleration, r_w is the tire radius, μ is the coefficient of rolling friction, θ is the grade angle, K_T is the torque constant of DC motor, $J_v = M_v r_w^2 / G^2$ is the equivalent inertia at the motor shaft, and G is the gear ratio which is one in in-wheel drive mode. Rolling resistance is the force that resists motion when a wheel rolls on a surface. It is mainly attributed to the rolling loss group including friction losses between the contact surfaces, wheel bearings loss, and the amount of deformation of the wheels or roadbed surface under various operating conditions. Bearings loss becomes a dominated factor in the case where the sliding bearings are considered. According to Manfred & Henning (2013), the coefficient of bearing friction remains a relatively small value at a high driving velocity, whereas it shows a high value at rest or a low driving velocity. Further, compared with rolling friction,

static friction is affected more by the varying hardness and roughness between the wheel and the road surfaces. The resistive torque acting on the wheel flange at the initial moment of start-up could reach several times greater than the rolling one (Wang et al., 2012). Consequently, a distinction between static and kinetic conditions should be taken into consideration during the start-up process.

MODELING OF START-UP PROCESS INVOLVING SUDDEN ENGAGEMENT OF THE CLUTCH

As a coupling component, which is placed between the master and slave sides of the drive train system, the clutch provides a transfer of power or torque to engage and disengage the driving motor from the wheel. Before the clutch engagement, the driving motor idles at no-load speed while the vehicle remains stationary. Then gradual wheel acceleration occurs with a non-zero engagement speed, and the corresponding dynamic process can be modelled as

$$\begin{aligned} J_e \omega_e &= T_c - T_c \\ J_v \omega_v &= T_c - T_L \end{aligned} \quad (4)$$

In the numerical and experimental measurements conducted in Ragupathy et al. (2016); Thorausch et al. (2009), the action of rapid clutch engagement always produces significant impulsive loads among the engine mounts and driveline components. In this case, it is assumed that the impulsive torque transferred through the clutch is far greater than the motor torque and the load torque. Acted upon by the clutch transfer torque T_c , the motor speed is decreased while the wheel speed is increased simultaneously at the time of clutch engagement. Once the rotational speed difference between the motor and the wheel approaches zero, the following equation can be derived from Equation (4),

$$t_c \frac{T_c}{J_v} = \frac{\omega_0 J_e}{J_e + J_v} \quad (5)$$

where t_c is the elapsed time for allowing the motor and the wheel to reach the same speed, and ω_0 is the no-load speed, the so-called idle speed. It shows that the final wheel speed after clutch engagement is simply affected by the idle speed.

In an engaged state, a fastened connection is achieved between two rotating masses, whereas zero force (or torque) is transmitted in a disengaged state. Analogous to ideal electrical switch, the ideal mechanical coupling between two rotating mass with different speeds engages and disengages instantaneously. Thus, the paper features an ideal coupling model between two masses having different rotating speeds and considers such an event as a completely inelastic collision. Correspondingly, the common speeds, while the clutch is locked, are calculated on the basis of the angular momentum conservation law (Buisson et al., 2002). The wheel is acquired with a speed of ω_1 after the clutch is instantly locked,

$$\omega_1 = \frac{\omega_0 J_e}{J_e + J_v} \quad (6)$$

It is implied from Equation (6) that the ideal coupling process agrees with the derived result described by Equation (5). The action of rapid clutch engagement of the master and slave sides can be considered to agree with engagement process of an ideal clutch model.

IMPLEMENTATION OF VARIABLE-IDLE SPEED CONTROL STRATEGY

Vehicle drivability is an important aspect for qualifying the driving comfort and shift quality of a vehicle. But its evaluation criterion is susceptible to driver's subjective perception. Previous studies have found that jerk (change rate of acceleration) is the key factor that relates the shift quality and ride comfort (Dovgan et al., 2012; Fuse et al., 2016). Excluding the influence of the vertical and horizontal vibrations caused by the uneven road conditions, most of researches quantify the starting or shifting performance of vehicle objectively by measuring the change rate of the vehicle's longitudinal acceleration, called jerk or shock intensity. So, jerk is used to reflect drivability performance in this study.

CONTROL OBJECTIVES

The aforementioned contents suggest that the clutch transmits the motor torque through the drive train to the wheel in the locked state, whereas the equivalent driveline loads via the operation of rapid clutch engagement. In order to avoid a sudden change in wheel acceleration at the moment of clutch closure, say \bar{t} , the proposed strategy, therefore, aims to assure a fast engagement without motor stalling and less shock intensity before and after speed synchronization of the motor and the wheel, through a suitable idle speed adjustment. Thus, the following requirements need to be considered,

- providing the requested motor torque at the moment of clutch closure \bar{t} to maintain a creeping or crawling speed of the wheel after clutch engagement.
- guaranteeing as small as possible the fluctuation of the wheel acceleration before the pre-synchronization and post-synchronization of the clutch.

INFLUENTIAL ELEMENTS ON THE PERFORMANCE INDICES

When starting the driving motor with load under the fastened connection, the peak current is governed by

$$I_{\max} = \frac{u_a}{R_a} \quad (7)$$

Differentiating Equation (2) with respect to time, the shock intensity when the driving motor starts at load under the fastened connection is described by

$$jerk = \frac{r_w}{J_v} \frac{dT_e}{dt} = \frac{r_w K_T}{J_v} \frac{di_a}{dt} \quad (8)$$

When applying the clutch start, kinetic energy stored in the master side will be transferred to the slave side during the clutch engagement process. As mentioned in Subsection 2.3, based on the ideal clutch model, the equivalent wheel acceleration can be calculated by applying the impulse-momentum equation,

$$\left| \frac{\Delta\omega_v}{\Delta t} \right| = \frac{\bar{T}}{J_v} \quad (9)$$

where Δt is the clutch engagement time, \bar{T} is the equivalent average torque, and $\Delta\omega_v$ is the angular velocity variation of the wheel.

Considering that the wheel accelerates from standstill, its angular speed variation is given by Equation (6). Substituting the wheel speed variation from Equation (6) into Equation (9), the equivalent wheel acceleration is acquired. Then, combined with the definition of jerk, the absolute value of the shock intensity, while the clutch engages instantaneously, is governed by

$$|a| = \frac{J_e}{J_e + J_v} \frac{r_w \omega_0}{\Delta t \times T_s} \leq Const \quad (10)$$

where T_s is the sampling period, and $Const$ is a positive constant to be chosen. The recommended value for the $Const$ is 10 m/s³ in German standards and 17.64 m/s³ in Chinese standards (Sun et al., 2015).

In practical applications, direct measurement of jerk is difficult to be realized. In general, shock intensity is obtained by differentiating the acceleration with respect to time. Since human beings are more sensitive to the low frequency oscillations in the range of (1014-) Hz (Hackl, 2011), the jerk calculation is therefore based on a filtered signal and can be acquired by differentiating the filtered acceleration by time interval.

On the other hand, acted upon by the clutch transfer torque during the rapid engagement of the clutch, the motor speed is linearly dropped based on the ideal clutch model. At the same time, the armature current increases from the ideal no-load current to the expected armature current. Ignoring the effect of armature

reaction, the output torque of DC motor is proportional to the armature current. Combining Equation (6), the output torque of the motor during the engagement process can be calculated by solving Equation (1) and Equation (2); thus the analytical expression of armature current is described as follows:

$$\begin{cases} i_a(t) = R_a^{-1}[(A + B\tau_a)(1 - \exp(-\frac{t}{\tau_a})) - Bt] \\ A = u_a - K_e\omega_0, B = K_e \frac{\omega_1 - \omega_0}{\Delta t} \end{cases} \quad (11)$$

where τ_a is the electromagnetic time constant.

DETERMINATION OF THE IDLE SPEED FOR ENHANCING PERFORMANCE INDICES

For a better understanding of the principle of idle speed control, two performance indices, with respect to the starting current and the jerk level, are introduced. Equation (10) and Equation (11) suggest that increasing the idle speed will result in the larger jerk level and the expanded torque capability when the engagement time is determined. Obviously, the driving comfort and the desired motor torque at the clutch closure time \bar{t} are the contradictory elements. Thus the objective of the proposed control method is naturally explained as follows: according to the load conditions, the idle speed adjustment is to find a balance between the desired output torque of the motor and the jerk reduction, i.e., to realize a fast clutch engagement that is to ensure a high comfort level with an expected driving torque at the moment of clutch closure. Incorporating the objectives stated above, the paper is to analyze the effect of the current overshoot on the shock intensity by the idle speed adjustment. The comprehensive evaluation index for quantifying the start-up performance can be presented as

$$\text{Index} = \frac{\Delta i_a}{I_N} + \frac{j_{\max}}{j_{\lim}} \quad (12)$$

Note that symbols with subscript N indicate nominal value, and j_{\lim} is the recommended jerk for preserving good driving comfort, j_{\max} represent the max value of jerk level during the start-up process, and Δi_a is the current overshoot. Lower starting current and smaller jerk are usually preferred. In case the desired motor torque is included into the optimization, a whole set of solutions results, according to different idle speeds.

PRINCIPLE OF OPTIMAL IDLE SPEED

Two different phases are distinguished for a typical engagement process of the clutch. An increase of the wheel speed is acquired during the time slot $[t_0, \bar{t})$, and t_0 is the time instant when clutch begins to be engaged. $a(t_0)$ represents the equivalent wheel acceleration based on an ideal coupling during the time slot $[t_0, \bar{t})$, whereas $a(\bar{t})$ represents the wheel acceleration at the moment of clutch closure.

When a negative wheel acceleration is acquired at the moment of clutch closure, i.e., $a(\bar{t}) < 0$, it will result in $|a(\bar{t}) - a(t_0)| > |a(t_0)|$. As a consequence, the larger absolute value of the jerk level is obtained at the clutch closure time \bar{t} , compared with the one at the moment when the clutch instantaneously engages. This follows from the consideration that the acceleration discontinuity is equivalent to an approximation of jerk for the same time interval.

Equation (11) indicates the output torque of the motor at clutch closure time rises with the given idle speed. Combining Equation (10), it is pointed out the wheel accelerations, respectively, at the moment of pre-synchronization and post-synchronization of the clutch increase with the idle speed. Thus, two conditions with regard to the different slope of wheel accelerations at the moment of pre-synchronization and post-synchronization of the clutch are, respectively, considered.

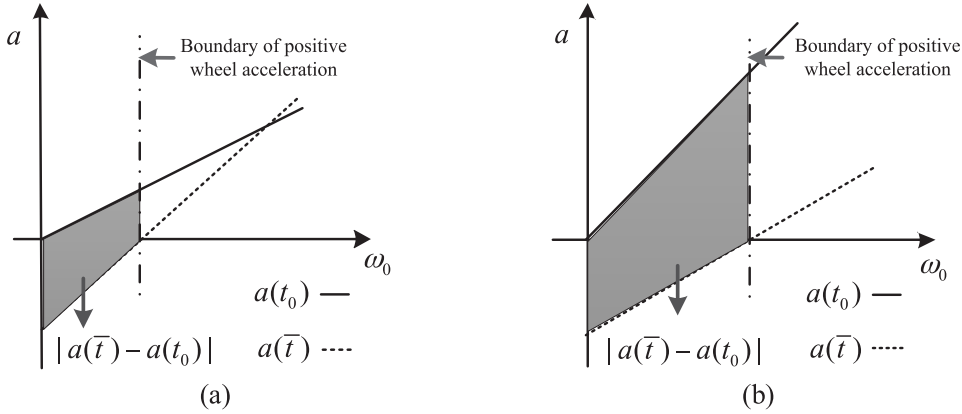


Figure 3. Graphical description of the wheel accelerations at the moment of pre-synchronization and post-synchronization of the clutch at different idle speeds: (a) the case with. (b) the case with.

$$\text{with } \frac{da(\bar{t})}{d\omega_0} > \frac{da(t_0)}{d\omega_0}. \text{ (b) the case with } \frac{da(\bar{t})}{d\omega_0} < \frac{da(t_0)}{d\omega_0}.$$

When the slope of $a(t_0)$ is lower than the one of $a(\bar{t})$, the absolute value of change in wheel accelerations at the clutch closure time decreases with the rise of the idle speed on the condition that the output torque of the motor at closure time \bar{t} is lower than the load torque,

$$|a(\bar{t}) - a(t_0)|_{\omega_0} > |a(\bar{t}) - a(t_0)|_{\omega_0 + \Delta\omega}, \text{ if } T_e(\bar{t}) < T_L \quad (13)$$

When the sufficient output torque of the motor is assured for continuous wheel acceleration at the moment of clutch closure, i.e., $a(\bar{t}) > 0$, it suggests the major jerk level during the start-up process is determined by the max changes in the wheel acceleration,

$$\Delta a_{\max} = \max(a(t_0), |a(\bar{t}) - a(t_0)|) \quad (14)$$

Its value changes with the rise of idle speed. Therefore, the minimum jerk will be acquired in this condition. The process can be explained in Fig. 3(a). The above analysis implies that any more improvements to the comfort level would be obtained with the further rise of the current overshoot. The given idle speed that corresponds to the sufficient output torque of the motor to match the load torque can be regarded as a Pareto equilibrium.

Another condition is illustrated in Fig. 3(b). It shows that the discontinuity in wheel accelerations at the moment of clutch closure rises with the idle speed. However, there is an apparent change with regard to the max acceleration discontinuity at critical boundary for assuring non-negative wheel acceleration. Similar to a two-point minimization technique, the offline optimization process about the idle speed adjustment can be understood as follows: provided that the adjacent difference of the jerk level is lower than a threshold value, the idle speed increment is continued. As long as the difference is larger than the threshold value, the idle speed increment is ceased and the corresponding speed can be considered as an optimal point under a working condition. Thus, this optimization process assures continuous wheel acceleration without bringing a fast increase of shock intensity.

EXPERIMENTAL SETUP AND RESULTS ANALYSIS

To validate the advantages of the clutch start and its principle of the idle speed selection, an experimental setup as shown in Fig. 4 is built for experimental research. The test bench is basically composed of four main systems: power unit (electric motor), control (operating arm), measurement (speed and torque transducer), and load (brake assembly + loading motor).

A 3 kW DC motor is selected for the power source of the whole driveline system. A speed and torque transducer is installed between the clutch mechanism and the driving motor, and it is used to measure the load torque and the rotational speed of the driving motor. A 30 kW DC motor serves as a generator and mimics the moment of inertia of a reference vehicle. The steady and dynamic loading can be controlled by the adjusting external resistance in series with the armature of the generator and the frictional force of the brake assembly, respectively. The specific DC motor parameters for experimental setup are listed in Table 1.

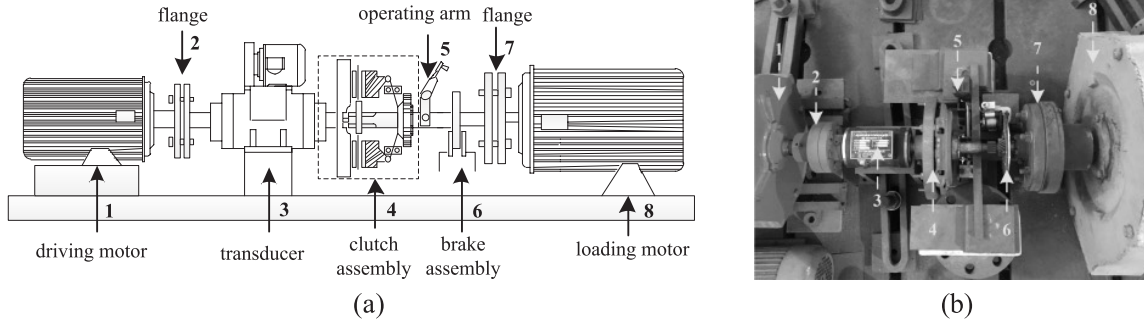


Figure 4. (a) Schematic diagram of the experimental setup. (b) Photograph of the test bench for simulating the load start-up in direct drive mode.

Table 1. Parameters of the DC motors for experimental setup.

Item	Symbol	Value
Driving motor		
Rated voltage	U_N	110 [V]
Rated current	I_N	35 [A]
Rated speed	n_N	750 [r/min]
Armature resistance	R_a	0.612 [Ω]
Filed voltage	U_f	220 [V]
Filed current	I_f	1.36 [A]
Motor inertia	J_e	0.6 [kg.m ²]
Loading motor		
Rated voltage	U_N	220 [V]
Rated current	I_N	159 [A]
Rated speed	n_N	1500 [r/min]
Load inertia	J_v	2.8 [kg.m ²]

Focusing on the investigations of the variable idle speed strategy, the paper primarily uses a mechanical clutch for the power transmission and interruption between the driving motor and the loading motor. When implementing the clutch start, the driving motor mounted on the master side is initially started to the expected rotational speed and holds it until the operating arm is quickly released. In this way, the impulsive loads that acted upon the driveline components can be produced via the rapid movement of the pressure plate when the motor idles at a certain speed. Accordingly, the impulse torque is applied on the loading motor and is equivalent to the variation in angular momentum of the slave side to the greatest extent.

Nevertheless, the transient loads can be caused in the driveline of the motor-clutch-load system via the operation of a sudden clutch engagement. Also, the dynamic loading is realized on the test bench above. The experimental setup is still appropriate for the studies on the control rule of the proposed method and verifying the effectiveness of the strategy.

COMPARISONS AND DISCUSSIONS

Generally, the average driving speed of an electric vehicle is about 50–60 km/h in consideration of the battery life and the urban drive cycle. So the input voltage of motor is restricted to 60 V for ensuring that the max load speed is around 50 km/h in experiments. The minimum idle speed of ICE is commonly in the range of 600–800 r/min, which is approximately 1/5–1/6 of maximum engine speed (Yuksel, 2011). Similarly, the no-load speed of the driving motor, which corresponds to 1/6 reference restricted voltage, is regarded as the fixed idle speed in subsequent experiments.

Firstly, the experiment on the direct start is performed. The given voltage across the armature is equal to the one that corresponds to the fixed idle speed. As shown in Fig. 5(a), the loading motor starts to rotate when the current approaches its peak value, which is about three times that of the steady-state current. It suggests that a starting condition with the static resistant moment, which is about three times as much as the steady state one, is considered.

Then, the clutch start is carried out at the fixed idle speed under the same load condition. Fig. 5(b) shows the loading motor is started quickly at the moment of clutch engagement while the armature current begins to rise to its peak value from the no-load current. Due to the different dynamic torques applied to the loading motor when the clutch suddenly engages, the load speed curve apparently shows different accelerating phases. It can be seen that the common speeds of the driving motor and the loading motor are acquired before the armature current reaching its peak.

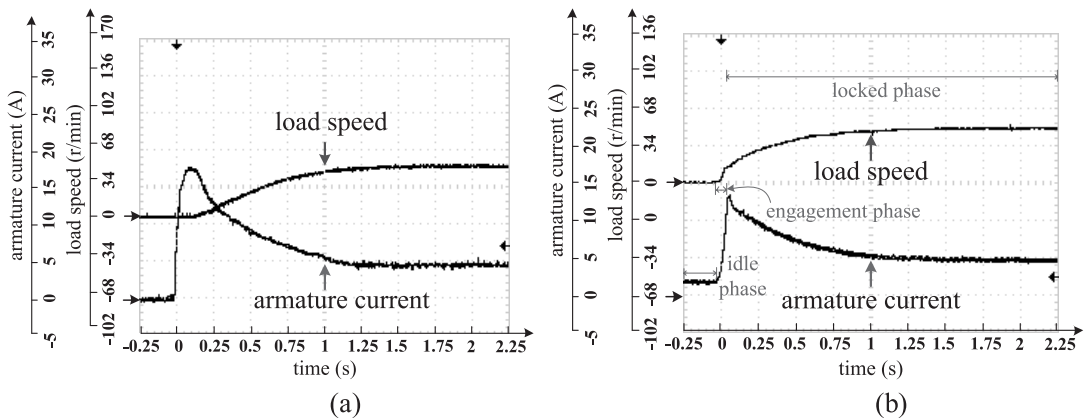


Figure 5. Scope captures of the direct start and the clutch start under same load condition: (a) the direct start with given armature voltage that corresponds to the fixed idle speed. (b) The clutch start at the fixed idle speed.

Accordingly, the contrast curves for the two start-up modes are shown in Fig. 6. In Fig. 6(a), the load speed is increased quickly during the clutch engagement process. Apparently, the moment when the loading motor accelerates from standstill is faster than the one by using the direct start. In contrast with the load start-up under the fastened connection, a quicker start-up process without motor stalling is achieved by using the clutch start. In Fig. 6(b), the peak value of armature current is approximately reduced by 25%, in contrast with the one by using the direct start. Because the loading motor remains still until the static resistance torque is overcome, the shape of the current curve by using the direct start is slightly concave-downward. By comparison, the current curve by using the clutch start is concave-upward response function, resulting from an initial speed acquired by the loading motor after rapid engagement of the clutch. However, the max jerk values displayed in Fig. 6(c) are almost same. There are no significant improvements for the performance indices only by applying the common scheme with a fixed idle speed control.

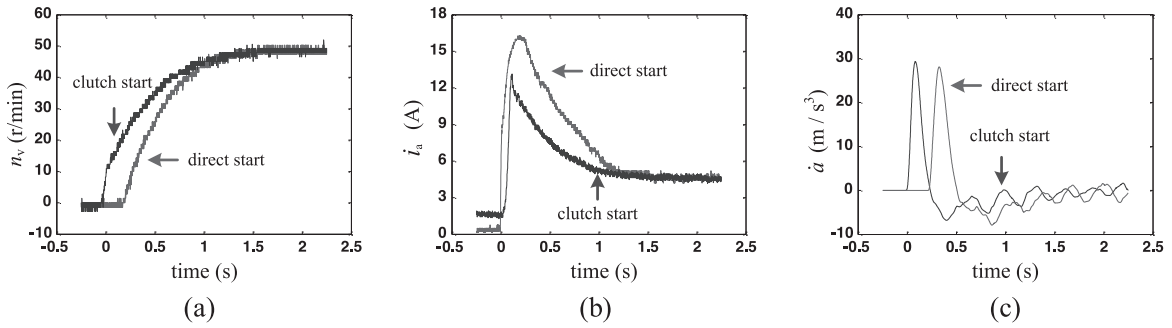


Figure 6. Comparisons of the direct start and the clutch start under same load condition:
 (a) load speed. (b) Armature current. (c) Jerk.

Subsequently, the same condition with the steady state load torque of 7 N.m is under discussion for the clutch start at variable idle speeds. The experimental curves between idle speed (n_0) versus transient angular speed at the moment of clutch closure (n_1), the peak current, and the jerk level are sequentially shown in Fig. 7. In Fig. 7(a), the velocity ratio before and after a rapid engagement of the clutch is roughly a constant, which is lower than the theoretical speed ratio based on the ideal clutch model. Similar to the proportional relation between the idle speed and the armature current from Equation (11), the experimental results as shown in Fig. 7(b) indicate that peak current increases with the idle speed linearly, and the peak value of the current is greater than the one in calculation data. It implies the loading motor is obtained with an initial speed after a fast clutch operation, and the obtained speed value is lower than the expected calculation value as well. In Fig. 7(c), it is noticed that the shapes of the plotted curves in either experiment data or calculation data are basically the same. The distinct changes are seen in the slope of the jerk curves; i.e., there exists an inflection point in each plotted jerk curve. Meanwhile, as indicated in Fig. 8, the motor torque at the clutch closure time equals the steady state load torque. Comprehensively, no more improvements to the jerk level will be achieved, where the undesired current overshoot is obtained by increasing the idle speed higher than 26 r/min. So, the no-load speed of the driving motor idling at 26 r/min can be interpreted as a Pareto-optimal point.

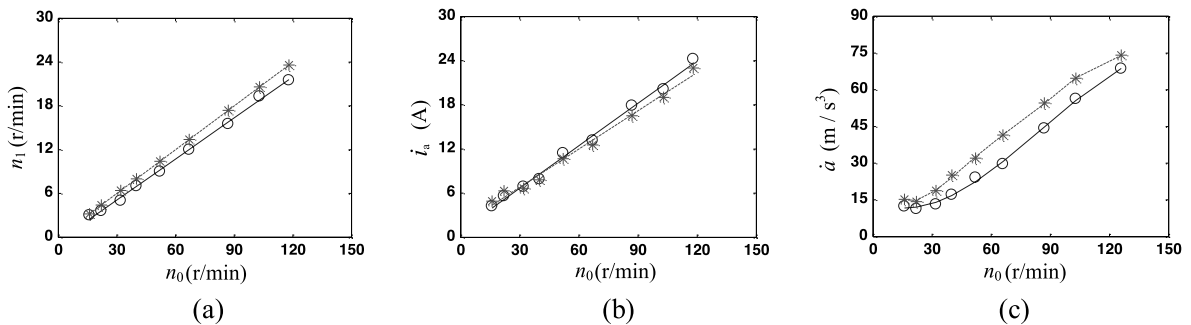


Figure 7. Relations between idle speed versus transient angular speed at the moment of clutch closure, peak current, and jerk (dotted line: the calculation data based on ideal clutch model; solid line: the experimental data): (a) speed. (b) Armature current. (c) Jerk.

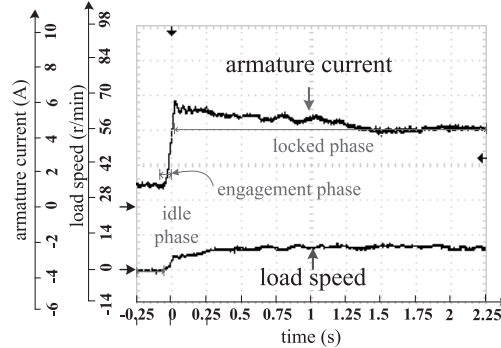


Figure 8. Scope capture of clutch start when the clutch engages at 26 r/min.

Next, the comparisons of performance indices between the clutch start with or without idle speed optimization are shown in Fig. 9. As shown in Fig. 9(a), the continuous load acceleration is assured when the clutch engages at a speed of 26 r/min. The contrast results of the armature current and the jerk curves between the clutch start with or without idle speed optimization are shown in Fig. 9(b) and Fig. 9(c). In contrast, the starting performance by using the clutch start at a fixed idle speed is not desirable, where the peak current is approximately 2 times to the one by using the variable-idle speed control. Also, the moderate jerk level is obtained by using the clutch start at the fixed idle speed, whereas about 200% jerk reduction is realized by using the optimized idle speed.

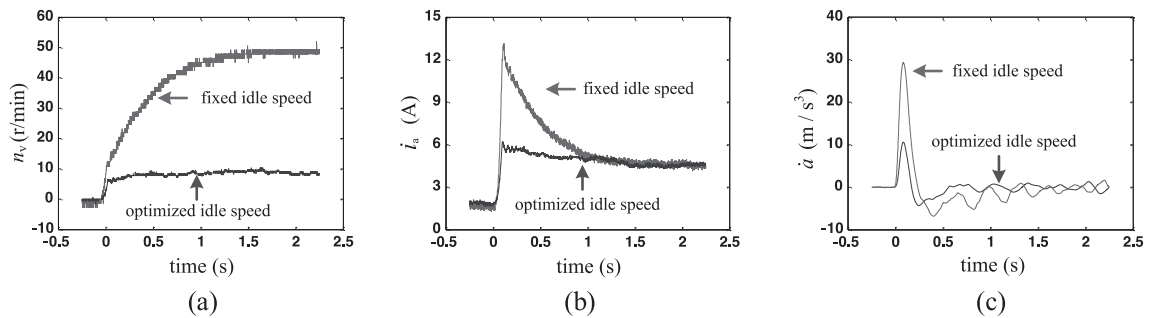


Figure 9. Comparisons of clutch start mode at fixed and variable idle speed under the same load condition:
 (a) load speed. (b) armature current. (c) jerk.

Overall, the mechanical and electromagnetic shocks are decreased by the idle speed adjustment according to the load torque in the case of small load conditions. It can be concluded the improved jerk level and the lower starting current will be obtained as long as the per-unit value of the starting torque does not exceed the one of the locked-rotor torque, which is determined by the initial given armature voltage that relates to the fixed idle speed.

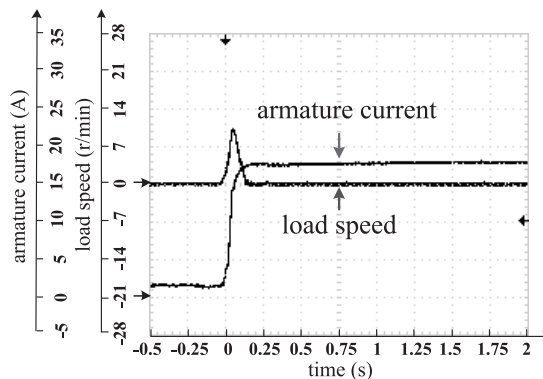


Figure 10. Scope capture of the clutch start when the clutch engages at the fixed idle speed under load torque 22 N.m. Subsequently, a condition with the steady state load torque of 22 N.m is investigated. Fig. 10 shows that a negative

acceleration of the loading motor occurs when the clutch engages at the fixed idle speed. As a result, the load speed is gradually decreased to zero. In spite of a moderate shock intensity when the clutch engages at the fixed idle speed, it leads to the restriction of motor torque at the clutch closure time.

Under the same load condition, as shown in Fig. 11(a) and Fig. 11(b), the start-up process of the load without motor stalling is realized by increasing the idle speed from 67 r/min to 103 r/min. In Fig. 11(c), although the shock intensity is increased to the higher level compared with the one at the fixed idle speed, enough power is acquired to assure a continuous wheel acceleration after the clutch is locked. However, Equation (8) suggests the factors that contribute to the jerk calculation include the constants like wheel radius, load inertia, and torque constant of the driving motor. On the other hand, the up-limit magnitude of the jerk level without undue discomfort in literatures (Lu et al., 2012; Sun et al., 2015) is applied to the vehicle occasions. Due to the fact the actual inertia of the whole drive train system is lower than the one of a typical light-weighted EV, therefore, the conversion coefficient should be taken into consideration to quantify longitudinal jerk under the existing test bench.

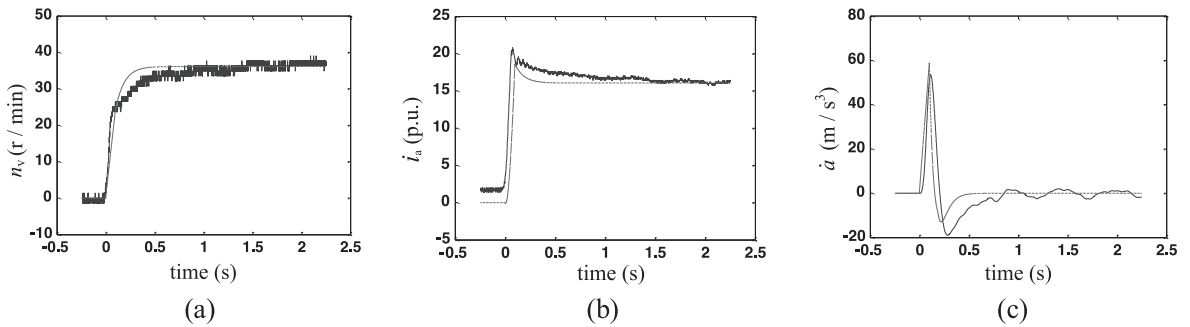


Figure 11. Experimental results of the clutch start mode when the clutch engages at 103 r/min (dotted line: the calculation data based on ideal clutch model; solid line: the experimental data):
 (a) load speed. (b) Armature current. (c) Jerk.

Considering that the weight of a compact EV is evenly distributed over the four wheels, the equivalent inertia referred to the motor shaft is about (18~22.5) kg.m² (a common case where the typical weight of light-weighted EV is about (800~1000) kg and the wheel radius is about 0.3 m). The inertia of the whole driveline (3.5kg*m²) on the laboratory test bench is approximately 20% of that in a typical light-weighted vehicle. So the jerk level for quantifying the driving comfort is scaled to approximately 20% of the calculated jerk value in experiment. Taking the conversion coefficient into account, the peak value of calculated shock intensity is not beyond the recommended jerk value. A smooth start-up without motor stalling is realized by implementing the proposed strategy.

The benefits of the clutch start by using the variable-idle speed control are studied. The results of the experiments performed on the existing test bench prove the rightness of the transverse comparisons between the clutch start and the direct start under the same load condition. Furthermore, it is concluded that the improved jerk level and the lower starting current are attained by the optimized idle speed selection. With the minimum jerk obtained by the adaption to the load torque at the corresponding idle speed, the curve through these idle speeds can be interpreted as Pareto-optimal solutions of the two performance indices optimization.

CONCLUSION

Moderate comfort level and restricted torque capacity are attained when the clutch engages at a fixed idle speed, which is a common case for the start-up of a traditional ICE vehicle. Instead, a start-up mode with optimal idle speed control is investigated in the paper. In contrast to the traditional fixed idle speed start-up mode, the experimental results using variable idle speed start-up mode show that the start-up jerk level and the peak armature current are approximately decreased by 67%. Moreover, the results indicate the improved torque capacity and the satisfactory jerk level can be achieved by tuning the idle speeds on the basis of the load torque. Further, in order to avoid the potential of the start-up failure when the clutch engages at the restricted idle speed for preserving a good driving comfort, future work will be extensively concentrating on improving torque capacity by compensating armature voltage during the engagement of the clutch.

ACKNOWLEDGMENT

This work was supported by The National Natural Science Foundation of China (51377063).

REFERENCES

- Chan, C.C., Bouscayrol, A. & Chen, K. 2010.** Electric, hybrid, and fuel-cell vehicles: architectures and modeling. *IEEE Transactions on Vehicular Technology*. **59**(2): 589–598.
- Sultana U., Khairuddin A., Rasheed N., Qazi S, Mokhtar A.S. 2018.** Allocation of distributed generation and battery switching stations for electric vehicle using whale optimiser algorithm. *Journal of Engineering Research*. **6** (3): 70-93.
- Xue, X.D., Cheng, K. & Cheung, N.C. 2008.** Selection of electric motor drives for electric vehicles. 2008 Australasian Universities Power Engineering Conference. Sydney, Australia.
- Larminie, J & Lowry, J. 2004.** Electric vehicle technology explained. John Wiley & Sons, Chichester. Pp.183–187.
- Heißing B & Ersoy M. 2011.** Chassis handbook: fundamentals, driving dynamics, components, mechatronics, perspectives. Springer, Berlin. Pp.42-44.
- Wen, H., Xiao, W., Li, H. & Wen, X. 2012.** Analysis and minimisation of DC bus surge voltage for electric vehicle applications. *IET Electrical Systems in Transportation*. **2**(2): 66–76.
- Jin, T.T., Li, P.K. & Zhu, G.M. 2013.** Optimal decoupled control for dry clutch engagement. 2013 American Control Conference. Washington, United States of America.
- Lu, T. L., Dai, F., Zhang, J. W. & Wu, M. X. 2012.** Optimal control of dry clutch engagement based on the driver's starting intentions. Proceedings of the Institution of Mechanical Engineers, Part D: Journal of Automobile Engineering. **226**(8): 1048–1057.
- Yuan, S.L. & Chen, L. 2013.** Model reference control to reduce both the jerk and frictional loss during DCT gear shifting. 2013 American Control Conference. Washington, United States of America.
- Zhong, K.M., Guo, P.Q. & Hu, B.C. 2000.** Centrifugal clutch with orthogonal force amplifier. *Chinese Journal of Mechanical Engineering*. **36**(4): 38–40,44.
- Asmis, N. & Schaffeld, W. 2012.** Advanced air management technologies for reducing fuel consumption and greenhouse gas emissions. SAE 2012 Commercial Vehicle Engineering Congress. Rosemont, United States of America.
- Cai, W. L., Gu, C. L. & Hu, X. D. 2015.** Analysis and design of a permanent magnet bi-stable electro-magnetic clutch unit for in-wheel electric vehicle drives. *Energies*. **8**(6): 5598–5612.
- Yu, W.G. & Gu C.L. 2017.** Dynamic analysis of a novel clutch system for in-wheel motor drive electric vehicles. *IET Electric Power Applications*. **11**(1): 90–98.
- Xiong, P. & Gu, C.L. 2014.** Optimal idling speed control of direct-drive electric vehicle launch in consideration of drive comfort. 2014 17th International Conference on Electrical Machines and Systems. Hangzhou, China.
- Matsushima, H. 2010.** Development of a control method to reduce acceleration shock in motorcycles. *SAE International Journal of Passenger Cars - Mechanical Systems*. **3**(2): 38–44.
- Manfred, M & Henning, W. 2013.** Dynamik der Kraftfahrzeuge. Berlin: Springer. Pp.15-17.
- Wang L., Liu J.L. & Wu X.G. 2012.** Research on starting capacity of lunar rover in extreme environment. *Journal of Southeast University (Natural Science Edition)*. **42**(suppl.1): 196–202.
- Braithwaite, E.R. & Greene, A.B. 1978.** Critical analysis of the performance of molybdenum compounds in motor vehicles. *Wear*. **46**(2): 405–431.
- Thorausch, M., Kirchner, E., Scheuermann, M., Babbick, T. & Sauer B. 2009.** Assessment method for passenger car transmissions under abusive loads. *ATZ worldwide*. **111**(1): 40–46.
- Ragupathy, R., Pothiraj, K., Chendil, C., Kumar P. T. & Vasudevan, P. 2016.** Powertrain Torsional Impact Load Causes, Effects and Mitigation Measures in a Parallel Mild Hybrid Powertrain. SAE 2016 World Congress and Exhibition. Detroit, United states.
- Buisson, J., Cormerais, H. & Richard, P.Y. 2002.** Analysis of the bond graph model of hybrid physical systems with ideal switches. Proceedings of the Institution of Mechanical Engineers, Part I (Journal of Systems and Control Engineering). **216**(1): 47–63.

- Dovgan, E., Tusar, T., Javorski, M. & Filipic, B. 2012.** Discovering comfortable driving strategies using simulation-based multiobjective optimization. *Informatica*. **36**(3): 319–326.
- Fuse, H., Kawabe, T. & Kawamoto, M. 2016.** A generation method of speed pattern of electric vehicle for improving passenger ride comfort. *Proceedings of the 13th International Conference on Informatics in Control, Automation and Robotics*. Lisbon, Portugal.
- Sun, J., Xing, G.J., Xing, Liu, X.D., Fu, X.L. & Zhang, C.H. 2015.** A novel torque coordination control strategy of a single-shaft parallel hybrid electric vehicle based on model predictive control. *Mathematical Problems in Engineering*. doi:10.1155/2015/960678.
- Hackl, T. 2011.** Innovative servo synchronizer and dog clutch technology for commercial vehicle MT, AMT and DCT Application. 2011 TM Symposium China. Shanghai, China.
- Yuksel, F. & Yuksel, B. 2004.** The use of ethanol-gasoline blend as a fuel in an SI engine. *Renewable Energy*. **29**(7): 1181–1191.

دراسة تجريبية للتحكم في سرعة تباطؤ عجلة قيادة مركبة كهربائية

بينغ شيونغ، ششينغلين غو

معهد الدولة لأبحاث الطاقة الكهربائية - هوبي، وجامعة هواتشونغ للعلوم والتكنولوجيا، ووهان الصين

الخلاصة

تم دمج نوع جديد من جهاز القابض (الدبرياج) في عجلة قيادة قطار يعمل بمركبة كهربائية رباعية الدفع للحصول على اتصال مرن بين المحور والمحرك. على عكس محرك الاحتراق الداخلي (ICE) الذي يتميز بأقل سرعة دوران، فإن المحرك الكهربائي قادر على التباطؤ بسرعات متغيرة. بعد ذلك، تم اقتراح نمط لبدء تشغيل نظام الدفع الرباعي الجديد، والذي يفصل بين بدء المحرك وتشغيل الحمل. أولاً، تم دراسة نموذج مبسط لنظام عجلة قيادة القطار، وتم تقديم مؤشرات الأداء لتقييم بدء تشغيل المركبة. بعد ذلك تم التحقق من طريقة البدء المقترحة، وتم ضبط سرعة التباطؤ على النحو الأمثل لإيجاد توازن بين انقطاع تسارع العجلة والعزم المطلوب لدوران المحرك في لحظة إغلاق القابض. وأخيراً، تم إجراء التجارب مخبرياً، وأثبتت النتائج تحسن ملحوظ في قدرة عزم الدوران من خلال تطبيق استراتيجية التحكم في السرعة المتغيرة للتباطؤ، مقارنةً بالنتائج التي تم الحصول عليها باستخدام التحكم في السرعة الثابتة للتباطؤ.